

# Ensemble Projection of the Sea Level Rise Impact on Storm Surge and Inundation in the Coastal Bangladesh

Mansur Ali Jisan<sup>1</sup>, Shaowu Bao<sup>1</sup>, Leonard J. Pietrafesa<sup>1</sup>

<sup>1</sup>Department of Coastal and Marine Systems Science, Coastal Carolina University, Conway, South Carolina, United States.

*Correspondence to:* Mansur Ali Jisan (mjisan@g.coastal.edu)

## Abstract.

The hydrodynamic model Delft3D is used to study the impact of Sea Level Rise (SLR) on storm surge and inundation in the coastal region of Bangladesh. To study the present-day inundation scenario, the tracks of two known tropical cyclones (TC) were used: Aila (Category 1; 2009) and Sidr (Category 5; 2007). Model results were validated with the available observations. Future inundation scenarios were generated by using the strength of TC Sidr, TC Aila and an ensemble of historical TC tracks but incorporating the effect of SLR.

Since future change in storm surge inundation under SLR impact is a probabilistic incident, that's why a probable range of future change in inundated area was calculated by taking in-to consideration the uncertainties associated with TC tracks, intensities and landfall timing.

The model outputs showed that, the inundated area for TC Sidr, which was calculated as 1860 km<sup>2</sup>, would become 31% higher than the present-day scenario if a SLR of 0.26 meter occurs during the mid-21<sup>st</sup>-21<sup>st</sup>-century climate scenario. Similar to that, an increasing trend was found for the end-of the 21<sup>st</sup>-century climate scenario. It was found that with a SLR of 0.54 meter, the inundated area would become 53% higher than the present-day case.

Along with the inundation area, the impact of SLR was examined for the changes in future storm surge level. A significant increase of 13.72% was found in storm surge level for the case of TC Sidr in Barisal station if a Sea Level Rise of 0.26 meter occurs at in the middle of the 21<sup>st</sup>-century. Similar to that, an increase of 28.67% was found in storm surge level with a SLR of 0.54 meter in this location for the end-of the 21<sup>st</sup>-century climate scenario.

Ensemble projections based on uncertainties of future TC events also showed that, for a change of 0.54 meter in SLR, the inundated area would range between 3500-3750 km<sup>2</sup> whereas for present-day SLR simulations it was found within the range of 1000-1250 km<sup>2</sup>

These results revealed that even if the future TCs remain at the same strength as at present, the projected changes in SLR will generate more severe threats in terms of surge height and the extent of inundated area.

## 33 1. Introduction

34

35 In addition to routine inundation from upstream river water and the downstream tides, the coastal part of Bangladesh is frequently  
36 flooded by storm surges induced by tropical cyclones (TCs). Typically, TC-induced storm surges in this area initiate in the central  
37 or southern part of the Bay of Bengal or near the Andaman Sea. TCs normally occur during April – May, the pre-monsoon period,  
38 and again from October – November, the post monsoon period. Harris (1963) mentioned that five basic processes (i.e., pressure,  
39 direct wind, earth's rotation, waves and rainfall effects) cause water level rise under storm conditions. Pietrafesa *et al.* (1986) also  
40 pointed out that high water at the mouths of coastal estuaries, bays, and rivers can block discharges of upstream waters and  
41 contribute to upstream flooding; a non-local effect. Among these processes, storm surges form primarily due to the TC wind  
42 stresses mechanically driving the surface frictional layer onshore. Assuming an idealized balance between pressure gradient force  
43 and surface wind stress with assumed small bottom stress, the surge related to TC wind stress can be expressed as  $\Delta\eta = \frac{\tau_w L}{g\rho h}$ , where

44  $L$  is the fetch of the wind (the distance over which the wind blows),  $\tau_w$  is the wind stress due to the friction between the moving air  
45 and water surface,  $g$  is the gravity,  $\rho$  is the density of water,  $h$  is the depth near the coast (Hearn, 2008). Also, as a secondary  
46 process, due to the differences in pressure level, the water level rises in the areas of low atmospheric pressure and falls in the areas  
47 of high atmospheric pressure, which is how the rising water level offsets the low atmospheric pressure to keep the total pressure  
48 constant (Harris *et al.*, 1963).

49 According to Murty *et al.* (1986), the surge amplifies as it approaches the coast due to the shallow continental shelf of the Bay of  
50 Bengal and hence it causes massive flooding in the low-lying coastal areas. A large percentage of the Bangladesh population  
51 resides in the ~~low-lying~~ coastal regions of the country. Most of the areas near the coastal zone of Bangladesh have been formed  
52 by the process of riverine sedimentation and because of that the ~~low-lying~~ areas are relatively flat and as such are susceptible  
53 to flooding even under normal astronomical tide conditions. Furthermore, the triangular shape of the Bay of Bengal region makes  
54 storm surges more distressing, as a funneling effect occurs. The geomorphological characteristics of the region have made the  
55 ~~coastal~~ prone to major TC events, events which have occurred multiple times in the past, directly causing ~~loss the deaths of~~  
56 ~~hundreds of thousands~~ of lives (Haque, 1997). ~~This type of coastal flooding associated with the changes in coastal water level due~~  
57 ~~to storms passing over the sea causes great loss of human lives~~, property, livelihoods and the economy of the country (Haque,  
58 1997).

59 Future climate change scenarios may further exacerbate the threats of TC-induced storm surge and inundation. According to the  
60 Intergovernmental Panel on Climate Change Fourth Assessment Report (IPCC 4AR), there is a high probability of major changes  
61 in TC activity across various ocean basins including the Arabian Sea and the Bay of Bengal. According to Milliman *et al.* (1989),  
62 this Ganges-Brahmaputra-Meghna Delta region has long been characterized as a highly vulnerable zone due to its exposure to the  
63 increasing trend of SLR. According to the SLR analysis done by the South Asian Association for Regional Cooperation based on  
64 the 22-year records of observed sea level at Charchanga, Cox's Bazar and Hiron Point, sea level is rising at rates of 6.0, 7.8 and 4  
65 mm/year, respectively in those three locations (SMRC, 2003). These rates are much higher than the global rate of SLR (~ 3.2  
66 mm/year) over the last 25 years (Pietrafesa *et al.*, 2015). Based on Warrick *et al.* (1996), the sea level in the Bay of Bengal is also  
67 influenced by local factors including tectonic setting, deltaic processes, and sediment load; for example, the coastal region of  
68 Bangladesh has been subsiding due to the pressure on the Earth's crust from the sediment with thick layers that have formed over  
69 millions of years. Warrick *et al.* (1996) also analyzed the recent history of land accretion and suggested that the subsidence is also  
70 balanced by land accretion due to sediment supply from the coast. These physical phenomena have been shaping the coast of

71 Bangladesh over the past 100 years. A global SLR of 26-59 cm has been projected over the next 84 years to 2100 by the IPCC  
72 under the scenario A1F1 (Meehl et al. 2007). In this proposed work, we will use the SLR projections from Caesar et al. (2017;  
73 under review), which is based on IPCC AR5 and suggests a projection of SLR of 26 cm for the mid-21<sup>st</sup>-century (2040 -2060) and  
74 54 cm for the end-21<sup>st</sup>-century (2079 -2099).

75 Previous studies have analyzed the likely impact of climate change, especially SLR, on storm surge and inundation in this region.  
76 Using hydrodynamic models, Ali (1992) showed that with an increase of 1.0 and 1.5 metersm of SLR, 10% and 15.5%,  
77 respectively, of the entirety of Bangladesh would get flooded under the strength of future TCs. Karim and Mimura (2008) used a  
78 1-D hydrodynamic model to study the inundation under several scenarios of climate and for the case of future TCs by changing  
79 sea surface temperature, SLR, wind speed and sea level pressure. Based on their results, Karim and Mimura (2008) concluded that  
80 with an increase of 2°C in SST and 0.3 metersm of SLR, the flood risk area would be 15.3% more than the present-daypresent-day  
81 risk area and the depth of flooding would increase by as much as 22.7% within 20 km from the coastline. Both Ali (1992) and  
82 Karim & Mimura (2008) considered SST rise and future strength of TCs in simulating the future storm surge and inundation.

83 However, the impacts of climate change on the frequency and intensity of TCs are still debatable (Knutson *et al.*, 2010). The  
84 projection of the TC characteristics in the Bay of Bengal region is unclear as well. To improve these uncertainties, a reasonable  
85 method to examine the impact of future SLR on storm surge and inundation would be to construct an ensemble of tracks and  
86 intensities of possible land-falling TCs along the Bangladesh coast based on the historical TC records. From this statistical  
87 approach, we can quantify the probable impact of TC tracks under future SLR change. To date, such an approach has not been  
88 done and will be the method of this study.

89 We first use Delft3D to simulate the present-daypresent-day storm surge and inundation using the strength of two recent TCs (TC  
90 Sidr and TC-Aila) and validate the simulations with observational data. Future storm surge and inundation scenarios were then  
91 generated by incorporating the projected SLR.

92 The study was carried out in the Ganges-Brahmaputra-Meghna Delta regions (Figure 1a). According to Integrated Coastal Zone  
93 Management Plan, 19 districts of Bangladesh located near the Bay of Bengal area were defined as the coastal areas. We've  
94 considered all those in this study. We selected two TC cases in this study, a strong Saffir-Simpson(SS) Category-5 that directly hit  
95 the study area, TC Sidr, and the other a SS-Category -1 storm that made landfall in the South West-southwest part of the study  
96 domain, TC Aila.

97 TC Sidr made landfall near Barguna district (Figure 1a) in 2007, causing ~ 3000 human fatalities and leaving millions homeless.  
98 This categoryCategory-5 cyclone is considered one of the most powerful cyclones in the past 15 years to have made landfall in  
99 Bangladesh, which affected over nine million people living aeross-in the Bangladesh coastal areas. The districts of Patuakhali,  
100 Khulna, Barguna and Jhalokathi were badly affected. During TC Sidr, around 15% of the affected people took refuge in nearby  
101 cyclone shelters. In the village of Angul Kata in Barguna district, around 1500 people took shelter in eight reinforced pillars to  
102 protect themselves from the tidal surge of around 5 metersm. If there had been no shelters, the death toll could have reached into  
103 the hundreds in that area.

104 The other cyclone studied in this paper, TC Aila (Figure 1a) occurred in the Bay of Bengal region in 2009. Although a  
105 categoryCategory-1 storm, Aila caused ~ 190 deaths and affected 4.8 million people, the devastation that left a long-long-term  
106 impact. The locales mainly affected were Khulna, Patuakhali and Chandpur. The storm surge due to Aila broke a dam in  
107 Patuakhali and submerged five villages, destroying a huge number of homes and leaving thousands of people homeless. Most of

the people living in those affected areas took shelter in the nearest cyclone shelters. According to government sources, approximately 2,500,000 houses had been destroyed completely and 3,700,000 houses had been damaged.

The structure of the paper is as follows: brief description of the Delft3D Flow model and the methodologies used to simulate future changes in storm surge and inundation, to generate ensemble projections of storm surge inundation were discussed in section 2. In section 3, validation of the model results, present day present-day storm surge inundation scenarios, ensemble projection of storm surge inundation and future change in storm surge level were presented. Section 54 includes discussion of model results and the uncertainties associated with the future projections. Finally, section 5 presents the concluding remarks on research findings.

~~TC Sidr made landfall near Barguna district (Figure 1) in 2007, causing 3000 human fatalities and leaving millions homeless. TC Aila occurred in the Bay of Bengal region in the year 2009 (Figure 1). Although a category 1 storm, Aila caused 190 deaths and affected 4.8 million people, devastation that left a long term impact. The locales mainly affected were Khulna, Patukhali and Chandpur. The storm surge due to Aila broke a dam in Pataukhali and submerged five villages, destroying huge number of homes and leaving thousands of people homeless.~~

## 2. Methodology

### 2.1 Modeling Methodology

#### 2.1.1 Application of Numerical Model

~~For the purpose of developing~~To develop a the present day present-day and future inundation scenario in the coastal regions of Bangladesh, the Delft3D-FLOW (Delft Hydraulics, 2006), a multidimensional (2D or 3D) hydrodynamic and transport simulation program that calculates non-steady flow and transport phenomena resulting from tidal and meteorological forcing was used. Delft3D-FLOW solves the unsteady shallow water equation in two ~~dimensions~~ (depth-averaged) or ~~in~~ three dimensions. The system of equations consists of the horizontal equations of motion, the continuity equation, and the transport equations for conservative constituents. The equations are formulated in orthogonal curvilinear ~~eo-ordinates~~ coordinates or in spherical ~~eo-ordinates~~ coordinates. Delft3D – FLOW module's two-dimensional, depth averaged flow equations can be applied for modeling tidal waves, storm surges, tsunamis, harbor oscillations (seiches) and transport of pollutants in vertically well-mixed flow regimes. In this paper Delft3D's 2D mode for barotropic depth-integrated flow has been applied. The equations are listed below.

$$\frac{\partial \zeta}{\partial t} + \frac{1}{\sqrt{G_{\xi\xi}\sqrt{G_{\eta\eta}}}} \frac{\partial [(d+\zeta)v\sqrt{G_{\eta\eta}}]}{\partial \xi} + \frac{1}{\sqrt{G_{\xi\xi}\sqrt{G_{\eta\eta}}}} \frac{\partial [(d+\zeta)v\sqrt{G_{\xi\xi}}]}{\partial \xi} = Q \quad (1)$$

$$\frac{\partial u}{\partial t} + \frac{u}{\sqrt{G_{\xi\xi}}} \frac{\partial u}{\partial \xi} + \frac{v}{\sqrt{G_{\eta\eta}}} \frac{\partial u}{\partial \eta} + \frac{uv}{\sqrt{G_{\xi\xi}\sqrt{G_{\eta\eta}}}} \frac{\partial \sqrt{G_{\xi\xi}}}{\partial \eta} - \frac{v^2}{\sqrt{G_{\xi\xi}\sqrt{G_{\eta\eta}}}} \frac{\partial \sqrt{G_{\eta\eta}}}{\partial \xi} - fv + \frac{g}{\sqrt{G_{\xi\xi}}} \frac{\partial \zeta}{\partial \xi} = -\frac{1}{\rho_0 P_{atm} \sqrt{G_{\xi\xi}}} \frac{\partial P_{atm}}{\partial \xi} + F_{\xi} \quad (2)$$

$$\frac{\partial v}{\partial t} + \frac{u}{\sqrt{G_{\xi\xi}}} \frac{\partial v}{\partial \xi} + \frac{v}{\sqrt{G_{\eta\eta}}} \frac{\partial v}{\partial \eta} + \frac{uv}{\sqrt{G_{\xi\xi}\sqrt{G_{\eta\eta}}}} \frac{\partial \sqrt{G_{\xi\xi}}}{\partial \eta} - \frac{u^2}{\sqrt{G_{\xi\xi}\sqrt{G_{\eta\eta}}}} \frac{\partial \sqrt{G_{\xi\xi}}}{\partial \eta} + fu + \frac{g}{\sqrt{G_{\xi\xi}}} \frac{\partial \zeta}{\partial \xi} = -\frac{1}{\rho_0 P_{atm} \sqrt{G_{\eta\eta}}} \frac{\partial P_{atm}}{\partial \eta} + F_{\eta} \quad (3)$$

where  $\xi$ ,  $\eta$  are the spatial ~~eo-ordinates~~ coordinates,  $\zeta$  is representing water level above some horizontal plane of reference (m),  $u$  &  $v$  are the velocities in the  $\xi$  and  $\eta$  direction (m/s),  $d$  is the water depth below some horizontal plane of reference (m),  $f$  is the coriolis forcing due to the rotation of the earth,  $g$  is the acceleration of gravity ( $m/s^2$ ),  $P_{atm}$  is the atmospheric pressure at water surface ( $kg/m/s^2$ ),  $Q$  is the discharge of water, evaporation or precipitation per unit area (m/s),  $\rho_0$  representing is the the density of

140 water,  $\sqrt{G_{\xi\xi}}$  is the coefficient used to transfer one coordinate system into another one (m),  $F_{\xi}$  are the turbulent momentum flux in  
 141  $\xi$ -direction ( $m/s^2$ ),  $F_{\eta}$  are the turbulent momentum flux in  $\eta$ -direction ( $m/s^2$ ). Along with the appropriate set of initial and  
 142 boundary conditions, the above-mentioned ~~set of~~ equations have been solved on an Arakawa-C type finite difference grid. Delft3D-  
 143 FLOW manual (Delft Hydraulics, 2006) contains detailed information about these numerical aspects.

### 144 2.1.2 Model Grid and Bathymetry

145  
 146 The grid was set up using spherical coordinates, ~~as displayed in Figure 1a.~~ The grid spacing varies from a minimum of 125  
 147 meters to a maximum of 1140 meters. The finer resolution ~~was~~ applied over land for calculating the inundation or wetting  
 148 process accurately.

149 In this study, the land topography data were obtained from NASA's Shuttle Radar Topography Mission (SRTM) 90-m resolution  
 150 datasets (Figure 1b). The bathymetries of the rivers and estuaries are specified using the cross sections measured by the Institute  
 151 of Water and Flood Management, Bangladesh. ~~The land elevations are specified using the data from the Center for Environmental~~  
 152 ~~and Geographic Information Services (CEGIS), Bangladesh.~~ The ocean bathymetry ~~was~~ specified using the data from the General  
 153 Bathymetric Chart of the Oceans 30-arc-sec interval gridded data (BODC, 2003, Figure 1b). Bathymetry and topographic data  
 154 ~~were have been~~ interpolated over the model domain using triangular interpolation and grid-cell averaging methods of Delft3D  
 155 (Delft Hydraulics, 2006).

### 156 2.1.3 Wind and Pressure Field

157  
 158 Track data of TCs Sidr and Aila were obtained from the Indian Meteorological Department ([www.imd.gov.in](http://www.imd.gov.in)). Using those data  
 159 as input, TC surface winds and mean sea level pressure fields were generated using the Wind Enhancement Scheme (WES)  
 160 (Heming et al. 1995) method based on the analytical equation by Holland (1980). Delft3D slightly improved the original WES by  
 161 introducing TC asymmetry. Unlike some ~~pervious-previous~~ method that incorporates TC wind asymmetry information from  
 162 observations (Xie et al. 2006), in WES the asymmetry was brought about by applying the translation speed of the cyclone center  
 163 displacement as steering current and by introducing rotation of wind speed due to friction (Delft Hydraulics, 2011, Heming et al.  
 164 1995).

165 According to the Holland's equation, gradient wind speed  $V_g(r)$  at a distance  $r$  from the Centre of the cyclone is expressed as the  
 166 following:

$$167 V_g(r) = \left[ \frac{AB(p_n - p_c) \exp\left(-\frac{A}{rB}\right)}{\rho r^B} + \frac{r^2 f^2}{4} \right]^{0.5} - \frac{rf}{2} \quad (4)$$

168 Here  $\rho$  is the density of air,  $p_c$  is the central pressure and  $p_n$  is the ambient pressure, the Coriolis parameter is represented by  $f$ .  
 169 A and B are determined empirically; with the physical meaning of A as the relation of pressure or wind profile relative to the  
 170 origin, and parameter B defining the shape of the profile. Delft3D introduces a central pressure drop of  $p_d = p_n - p_c$ . By equating  
 171  $\frac{dV_g}{dr} = 0$ , and assuming  $f=0$  in the region of maximum winds where the Coriolis force is small compared to the pressure gradient  
 172 and centrifugal forces, the radius of maximum winds  $R_w$  can be given as follows:

$$173 R_w = A^{1/B} \quad (5)$$

174 Thus,  $R_w$  is independent of the relative values of ambient and central pressure and is defined entirely by the scaling parameters A  
175 and B. Substitutions lead to the expression for the maximum wind speed  $V_m$

$$176 V_m = \left[ \frac{Bpd}{\rho e} \right]^{0.5} \quad (6)$$

177 Where  $e$  is the base of the natural logarithm (=2.71828182846).

178 Complete details about this method can be found in the user manual of Delft3D Flow (Delft Hydraulics, 2006), -Holland (1980),  
179 and Vatvani et al. (2002).

180 The circular grid of TC wind fields used in this study consists of 36 columns and 500 rows and the data were updated at 6 hourly  
181 intervals throughout its movement until the landfall. Figure 2 shows a snapshot of the wind field of TC Sidr over the model domain,  
182 before landfall, generated using Holland's equation above.

### 183 2.1.4 Roughness

184 The spatially varying Manning's Roughness value has been was defined based on land cover, such as vegetation, rivers, and ocean  
185 (Table 1). In the study domain, a mangrove forest, Sundarbans, is located in the Southwest region, near TC Sidr's landfall location  
186 (Figure 1a). Sakib et al. (2015) found that Sundarban plays a significant role as a buffer in reducing the total inundation during TC  
187 passages. Therefore, in this study, the mangrove region was considered.

188 In selecting the roughness values, methods described in Zhang et al. (2012) were as followed and slightly modified values were  
189 defined for the study area based on the vegetation types in that area.

### 190 2.1.5 Boundary conditions

191 Upstream boundaries were specified as discharges at the mouths of the three major rivers; the Ganges, the Brahmaputra & the  
192 Upper Meghna; obtained from the Bangladesh Water Development Board (BWDB) as daily discharge. The downstream ocean  
193 boundary was defined by the Topex/Poseidon Inverse Tidal model, based on Egbert et al. (1994) Location of the downstream  
194 ocean boundary is was shown in Figure 1a.

### 195 2.2 Calculation Procedure for Present Day Present-day and Future Storm Surge and Inundation Scenario

196  
197 To generate storm surge and inundation for present day present-day climate scenario, upstream discharge and downstream water  
198 level data from the present day present-day were used. For future SLR scenarios, present day present-day hydrodynamic conditions  
199 and the strengths of present day present-day TCs were used but the future sea level was modified based on the SLR projections by  
200 Caesar et al. (2017; under review). Scenarios were generated for both the Midmid-21<sup>st</sup>-21<sup>st</sup>-century and the Endend-21<sup>st</sup>-21<sup>st</sup>-  
201 century time horizons for these TCs, Sidr and Aila. Finally, comparisons were made in terms of storm surge and inundation to  
202 identify the changes between present day present-day and future SLR scenarios.

203 Now, future sStorm surge inundation due to SLR is a probabilistic event that requires proper addressing of the uncertainties  
204 associated with the input parameters. To address the future tropical cyclone uncertainties and obtain statistically significant results,  
205 we created an ensemble of tropical cyclone tracks. The ensemble tracks were generated from different historical tropical cyclones  
206 that made landfall over the study domain with different intensities (Table 2). Along with the uncertainties associated with future

207 landfall locations, the intensity of Sidr-like and Aila-like TCs may be different. So, to address the uncertainty with the intensity,  
208 we increased and decreased their intensity by 10% to simulate a probable range of future storm surge inundation.

209 Storm surge inundation can also be different based on landfall timing. If ~~the a storm would made~~ landfall during the high  
210 astronomical tide condition, its flooding would have been much higher at that time than what could happen during a low  
211 astronomical tide condition. For example, the tides shown in Figures 3 and 7 as the water level oscillations have amplitudes as  
212 high as 3 m, which could significantly affect the extension of flooded area, depending on whether the storm's landfall coincides  
213 with a high tide or a low tide. We note that TC Sidr and TC Aila made landfall during the high tide conditions, which may not  
214 always be applicable for the future TCs. To also address uncertainties with the TC landfall timing, experiments were conducted by  
215 changing the timing of landfall to identify the impact of high tide and low tide on storm surge and inundation. The change of timing  
216 in these tide-related experiments was implemented by modifying the tracks of the storms so that their landfalls coincide with a  
217 high tide, a tide, or a zero-tide condition, in addition to their actual tidal phases. Here in this study, future storm surge inundation  
218 scenarios caused by the ensemble tracks will then be simulated by incorporating the projected SLR. By taking all these parameters  
219 into consideration, we conducted a total 108 ensemble simulations (36 for each; ~~present day~~ and two SLR scenarios).  
220 Parameters that were considered in making ensemble projections are shown in Table 23.

### 221 3. Results

#### 222 3.1 Validation of the Model

223 Hourly tidal data from the Bangladesh Inland Water Transport Authority (BIWTA) was used to evaluate the performance of the  
224 model used in this study. The model simulation's root mean square error (RMSE)<sup>7</sup>, mean absolute error (MAE)<sup>8</sup> and dimension-  
225 less Nash-Sutcliffe coefficient (E)<sup>9</sup> (Nash and Sutcliffe, 1970) were calculated and listed in Table 43. A Nash-Sutcliffe coefficient  
226 ranges between negative (-ve) infinity (no skill simulation) and one (perfect simulation).

$$227 \quad RMSE = \sqrt{\frac{\sum_{i=1}^n (X_{obs,i} - X_{model,i})^2}{n}} \quad (7)$$

$$228 \quad MAE = \frac{1}{n} \sum_{i=1}^n |X_{obs,i} - X_{\hat{X}_{model,i}}| \quad (8)$$

$$229 \quad E = 1 - \frac{\sum_{i=1}^n (X_{obs,i} - X_{model})^2}{\sum_{i=1}^n (X_{obs,i} - \bar{X}_{obs})^2} \quad (9)$$

230 The simulated water levels were compared against the measured data from ~~Bangladesh Inland Water Transport Authority (BIWTA)~~  
231 at two locations: Barisal and Charchanga (Figure 1a). Barisal station is located more towards the inland whereas Charchanga is  
232 located near the coastline where the grid cell resolution was coarse. But none of them are in the open ocean water, which is  
233 important to get a clear idea about storm surge level. TC Sidr made landfall near the Barisal Station (Figure 1a) and the impact of  
234 the storm surge was clearer at the Barisal station than that of TC Aila, which made landfall outside the model domain (Figure 1a);  
235 therefore, its impact was not as clear as that of Sidr.

236 In Figure 3(a) for TC Sidr at the Barisal station, the modeled water level, including storm surge and astronomical tides, was slightly  
237 lower than the observations, and at the Charchanga station (Figure 3b) the measured water level variation displayed larger-smaller  
238 amplitudes than did the model outputs for positive tides and for negative tides, larger amplitudes than the modeled water level for  
239 negative tides, perhaps due to the coarse resolution of bathymetry. Similar types of variations between measured and modeled  
240 water level were found for TC Aila (Figure 3c and Figure 3d). Nevertheless, the modeled water level variations during TCs Sidr

241 and Aila agreed reasonably well with measured data; as also confirmed by the calculated average-RMSE, MAE and Nash-Sutcliffe  
242 coefficient(Table 4). Therefore, we conclude that the method can be used to study the impact of SLR on storm surge and inundation  
243 in future climate change scenarios.

### 244 3.2 Present Day Present-day Inundation Scenario

245

246 The storm surge inundation scenarios due to the two TCs considered are were shown in Figure 4.

247 It can be seen from Figure 4 that the area flooded by TC Sidr (yellow shade+red shade) was much higher than the area flooded by  
248 TC Aila (white shade+red shade), a result that is consistent with the fact that the category-5 TC Sidr was much stronger than the  
249 category-1 TC Aila and directly hit the study area. The maximum sustained wind speed for TC Sidr was 260 km/h whereas for TC  
250 Aila it was 110 km/h. The landfall location of Sidr was on the Eastern side of Sundarban, while for Aila, the landfall location was  
251 towards the Western side of Sundarbans. That explains why the inundations due to TC Sidr were located near the eastern side of  
252 Sundarban, whereas for Aila, the inundation was located mainly in the western part. The extent of inundation due to Sidr (1860  
253 km<sup>2</sup>) was 35% larger than that of Aila (1208 km<sup>2</sup>)

254 Sakib et al. (2015) showed that Sundarban acted as a buffer zone in reducing the impact of Sidr and thereby reduced much of the  
255 potential inundation depth and extent of flooding. As mentioned before, in the model simulation the impact of Sundarban was  
256 realized using a higher Manning's roughness value as resistance for the surge to travel.

### 257 3.3 Impact of Future Climate Scenarios on Storm Surge Inundation

258

259 Future inundation scenarios were generated for two different time horizons: one for the mid-21<sup>st</sup>-21<sup>st</sup>-century and the other for the  
260 end-of the-21<sup>st</sup>-century. The initial ocean water level was raised by 0.26 metersm and 0.54 metersm for the mid-21<sup>st</sup>-21<sup>st</sup>-century  
261 and end-21<sup>st</sup>-21<sup>st</sup>-century, respectively. The upstream river discharge and downstream ocean water level were used from present  
262 daypresent-day climate scenarios.

263  
264 In this section we seek to answer the question: if present daypresent-day's TCs were to happen in future SLR scenarios, what storm  
265 surge and inundation hazard would they cause? Therefore, the tracks and intensities of the two present daypresent-day TCs, Sidr  
266 and Aila, were used as the model wind input parameters.

267 The model simulated inundated areas and the percent variations were shown in Table 5 and Figure 5. Figure 5 shows that under  
268 future SLR scenarios, the inundated areas caused by TCs Sidr and Aila would be significantly higher than those under the present-  
269 day climate condition, as indicated by the white color shaded areas, for the TCs with the same strengths and landfall paths. For the  
270 category-5 TC Sidr, the inundated area would be 31% (2436.6 km<sup>2</sup>) and 53% (2845.8 km<sup>2</sup>) higher than present daypresent-day's  
271 1860 km<sup>2</sup> inundated area, in mid-21<sup>st</sup>-century-century (0.26 meterm SLR) and end-of-21<sup>st</sup>-century (0.54 meterm SLR) climate  
272 scenarios, respectively (Figure 5a and Figure 5b)

273 Similarly, for the category-1 TC Aila, a category 1 storm, there would be an increase in inundated areas. The calculated-simulated  
274 inundated areas for TC Aila under mid-21<sup>st</sup>-century-century and end-of 21<sup>st</sup>-century-century were was found to be 1550 km<sup>2</sup>  
275 (28.3%) square kilometers and 1770 km<sup>2</sup> (46.5%) square kilometers, respectively (Figure 5c and Figure 5d) whereas for the present-  
276 day scenario it was found to be 1208 km<sup>2</sup>.square kilometers.



277 ~~However in Figure 5, there are several small areas of yellow color indicating zones flooded under present conditions but not flooded~~  
278 ~~during future SLR conditions. This is because Figure 5 showed snapshots of the inundation conditions at one particular time. Some~~  
279 ~~areas may experience alternating wetting and drying conditions, which may explain why some areas are flooded with present SLR~~  
280 ~~and not with higher SLR: this is so only at that particular time. The authors expect that those areas are flooded at other times.~~

281  
282 All these simulations were ~~done~~carried out using the present-day tides, upstream river discharges and the TC tracks and strengths,  
283 with only the initial sea water level raised to reflect the effect of the projected future SLR. ~~of present day TCs; while changing the~~  
284 ~~initial sea water level to reflect the effect of SLR.~~ Therefore, the results suggest that even if the future TCs strengths, the tides, and  
285 river discharges remain the same as in the present-day climate condition, future SLR would significantly increase the inundated  
286 area, by as high as 53%.

287  
288 ~~All of these simulations were done using present day tides, river discharges and the track and strength of present day TCs; while~~  
289 ~~changing the initial sea water level to reflect the effect of SLR. Therefore, the results suggest that even if the future TCs strengths,~~  
290 ~~the tides and river discharges remain the same as in the present, future SLR would significantly increase the inundated area.~~

### 291 3.3.1 Ensemble Projection of Future Storm Surge Inundation under SLR Conditions

292 As discussed in section 2.2 ~~that, the~~ future change in storm surge inundation can be different based on the intensity, landfall location  
293 and timing of future TCs. By considering all ~~those~~these uncertainty factors mentioned in Table 23, a column plot was created  
294 (Figure 6) for ~~present-day~~present-day sea level and future SLR scenarios. Ensemble simulation outputs also showed an evidenee  
295 ~~forevident~~ increase in the inundated area under the effect of SLR. For the ~~present-day~~present-day scenario (black column), out of  
296 36 simulations, frequency of storm surge inundation incidents that would likely occur between the range of 1000-1250 km<sup>2</sup> is 13,  
297 whereas for 0.26 metersm of SLR (red column), peak of the column shifted towards right side with a maximum frequency of  
298 inundation events occurred within the range of 2000-2250 km<sup>2</sup> (10 times out of 36 simulation results). And for 0.54 metersm of  
299 increase in sea level (blue column), the peak of the column shifted more towards the right and the maximum number of simulation  
300 outputs (11 out of 36 simulations) showed the range of inundation to be within 3500-3750 km<sup>2</sup>. These results show that even the  
301 change in intensities of future TCs are indefinite and the landfall timing is uncertain, increase in sea level is going to increase the  
302 area of inundation.

### 303 3.4 Impact of Sea Level Rise on Future Storm Surge Level

304  
305 In addition to the inundation area, SLR would also greatly affect storm surge levels. Similar to the approach used in the inundation  
306 study (Section 3.3), TCs Sidr- and Aila-induced storm surges in the future SLR scenarios were simulated using their recorded  
307 strengths.

308 The simulated storm surge water levels in future SLR scenarios were compared with both the observed and model generated ones  
309 under the ~~present-day~~present-day scenarios (Figure 7). It is to be mentioned that, while generating the future water level under the  
310 effect of SLR, the baseline wasis only changeding by considering the SLR effect and based on that factor the future storm surge  
311 level was calculated. Other than that, the water level is the same as ~~present-day~~present-day TCs.

313 From Figure 7 we can see that for the case of TC Sidr the simulated storm surge level would become 2.13 meters (Figure 7a,  
314 Table 6) in Barisal station which is around 13.7224% higher than the present-day scenario. Similar to that, under the  
315 end-of-21<sup>st</sup>-century 0.54 meters SLR scenario in Barisal, the storm surge would be around 28.6737% higher (Figure 7a,  
316 Table 6) than the present-day scenario and the peak water level would reach 2.416 m (Table 6).

317 Increase in storm surge was found at the Charchanga station also. For TC Sidr, under the mid-21<sup>st</sup>-century scenario (0.26  
318 meter SLR), the model simulated storm surge level was found to be 13.9544% higher (1.87224 meters) (Figure 7b, Table 6)  
319 than the present-day and 33.4534% higher (2.1959 m) (Figure 7b, Table 6) than the present-day for the end-  
320 of-21<sup>st</sup>-century (0.54 m SLR) climate scenario. ~~It is to be noted that, there's a slight phase shift in the model simulation in~~  
321 ~~phase occurred forat this station during the period offrom November 13 to November 15. This could happen due to the presence~~  
322 ~~of seiche. However, for rest of the period, phase variations are similar to the observed ones.~~

323 For TC Aila in Barisal, the Storm Surge would become 21.932% higher than the present-day, which was 1.29964  
324 meters under the 0.26 meters SLR condition for the mid-21<sup>st</sup>-century climate scenario (Figure 7c, Table 7). During the  
325 end-of-21<sup>st</sup>-century climate scenario, the increment would become even higher as the SLR would be 0.54 meter. Storm  
326 Surge would be 50.964% higher (1.96 meters) (Figure 7c, Table 7) than the present day under the 0.54 meters SLR condition  
327 at the end of the century.

328 At Charchanga, the storm surge would be higher than the present-day condition for TC Aila. For the mid-21<sup>st</sup>-century-  
329 century under the 0.26 meters SLR scenario, the storm surge would become 3.0754 meters which is around 2350% higher  
330 than the present-day condition (Figure 7d, Table 7). And for the end-of-21<sup>st</sup>-century, this would become 5568% higher  
331 (3.875 m) than the present day as the SLR would reach 0.54 m (Figure 7d, Table 7).

332 ~~In order to analyze the linearity/non-linearity of storm surge level with respect to SLR, we conducted additional experiments~~  
333 ~~based on 5 SLR scenarios: present-day sea level, 0.26 m of SLR, 0.33 m of SLR, 0.4 m of SLR, 0.47 m of SLR, 0.54~~  
334 ~~m of SLR, respectively. Results from these experiments are presented in the Figure 8.~~

335 ~~For the case of TC Sidr in Barisal and Charchanga station, storm surge level increased almost linearly with respect to the addition~~  
336 ~~of water due to the effect of SLR. For example, with a SLR an SLR of 0.47 meters, the increase of storm surge level with respect~~  
337 ~~to present day in Barisal and Charchanga stations were 0.453 m and 0.445 m, respectively (Figure 8a). On the other hand for the~~  
338 ~~case of TC Aila, with a SLR an SLR of 0.26 meters, the increase in storm surge level were found 0.285 m and 0.575 m respectively~~  
339 ~~for the Barisal and Charchanga station (Figure 8b). Though the storm surge level is increasing almost linearly with the addition of~~  
340 ~~sea water, however, there's are still differences found between them, which could be influenced by the modification~~  
341 ~~of ocean bathymetry to incorporate the effect of SLR. The margin of differences is higher for the Charchanga station comparing it~~  
342 ~~with the Barisal station. The coarse resolution of topography near that area might be responsible for that.~~

343 ~~The 0.26 m SLR for the mid-21<sup>st</sup>-century would increase the water level, and the surge peak would be much higher at 2.4 m than~~  
344 ~~the present-day observed value at 2.0 m (Figure 7a). Figure 7b shows the same comparison, but for a 0.54 m SLR in the end-of-~~  
345 ~~21<sup>st</sup>-century scenario. For this case, the difference between the present day and end-of-21<sup>st</sup>-century peak water level is much higher~~  
346 ~~than what we found in the mid-21<sup>st</sup>-century climate scenario.~~

347

#### 348 4. Discussions

#### 349 4. Discussions

350 In this paper, we showed that even if the future TCs ~~keep remain~~ the same strength like the ~~present day present-day~~ ones their impact  
351 will be much higher in a changing climate due to the effect of SLR. Several other factors not included in the modeling could make  
352 the storm surge and inundation situation far worse than that shown in the modeling result. These factors include mangrove coverage  
353 decrease, morphological changes, TC strength increase, and upstream river discharge changes.

354 For including the effect of future SLR in the model simulations, several methodologies were examined. One of the methods with  
355 ~~which that~~ we experimented in this study was to include the increased sea level in open ocean boundary instead of adding it in to  
356 the whole ocean depth by keeping the coastline fixed. This method was used by some previous studies (Pickering et al. 2012).  
357 However, in such a case, an additional pressure gradient force was found acting towards the coast which made the inundated area  
358 much higher. Therefore, this method was not used in this study. Instead, in this study, the future SLR was added to the whole  
359 ocean domain depth.

360  
361 ~~In order to~~ make the future SLR simulation realistic, we considered the increased sea level in ocean bathymetry and increased  
362 the depth by 0.26 and 0.54 m, respectively, by considering land submergence near the coast. In that case, the result looked much  
363 more realistic than the previous one and this is the method we followed in this paper. For example, for the case of TC Aila under  
364 the end-of-21<sup>st</sup>-21<sup>st</sup>-century scenario where we used ~~a SLR an SLR~~ of 0.54 m SLR at the open ocean boundary instead of adding it  
365 to ocean depth and using the hydrodynamic conditions from the present day, the total inundated area was found to be 79% higher  
366 than the ~~present day present-day~~ one. Similar to that, for the mid-21<sup>st</sup>-21<sup>st</sup>-century scenario (a 0.26 m SLR), the inundated area was  
367 found to be 69% more than the ~~present day present-day~~ scenario. But when we added the SLR in ocean depth, the mid-21<sup>st</sup>-~~century-~~  
368 ~~century~~ and end-of-21<sup>st</sup>-~~century-century~~ inundated area were found to be 28% and 46% higher than the ~~present day present-day~~  
369 scenario. This increase in inundated area was much less than the one that we found by adding the SLR in the open ocean boundary.  
370 Figure 89 displays the differences in the inundated area based on the consideration of SLR in the model input.

371 As discussed earlier, TC Sidr made landfall near Sundarban, where the mangrove forest zone acted as a buffer in reducing the  
372 impact of the storm surge flood. That is why, even though it was a TC 5, its impact was not as high as it might have been expected  
373 to be. In this study, the roughness of the mangrove forest zone on the South-West part of Bangladesh was considered to be fixed  
374 for the ~~present day present-day~~ as well as for future scenarios. But Mukhopadhyay et al. (2015) predicted that 17% of the total  
375 mangrove cover could disappear by 2105. If this decreasing trend of vegetation were considered in this study, the flooded area  
376 could be much higher.

377 Morphological changes were not considered in this study. But according to Goodbred et al. (2003), each year the eastern-~~estuary,~~  
378 ~~the central estuary~~ and ~~the western estuarie~~s are losinglose land at a rate of 0.13 cm/year, 0.16 cm/year and 0.16 cm/year,  
379 respectively. This could also lead to increased inundated areas for future scenarios. But as the focus of the paper is to estimate  
380 ~~predict~~ the future scenario of storm surge and inundation due to the effect of SLR and to compare comparisons with the ~~present~~  
381 ~~day present-day~~ scenarios, it is important that we keep the roughness and morphological changes constant so that consistent  
382 comparisons can be made.

383 Some previous research showed that there could be increases in hurricane strength and landfall probability in the future due to  
384 global climate change (Haarsma et al. 2013, Bender et al. 2010, Bengtsson et al. 2007). Though we slightly modified the present-  
385 day TC strengths and selected 12 historical TC tracks to reduce landfall uncertainties and to make ensemble projection of future

386 storm surge inundation, strength may be much higher than the ones that we considered for this study. In such case, the devastation  
387 could well be much higher under projected SLR conditions, which is very alarming

388 In this paper, we used the present-day river discharge data as an upstream boundary for generating future inundation scenarios.  
389 But using the INCA-N, an Inland Catchment Modeling system and considering the projected climatic ~~&-and~~ socio-economic  
390 scenarios, Whitehead et al. (2015) showed that, there ~~will-would~~ be a significant increase in future monsoon intensities due to the  
391 impact of climate change. That would make future flooding scenarios much worse than those experienced presently. So, based on  
392 the changes in TC intensity, river discharges, and land-use changes, the situation could well become more badly impacted than  
393 what we found in this study.

394 The findings of our study are important for local governments to consider while they make new management and policy decisions  
395 and to improve TC preparedness plans by increasing numbers of shelters and heights. ~~Generally, i~~In TC shelters, the first floor ~~is~~  
396 ~~should be~~ kept ~~above the transparent due to the risk of~~ high surge waters. Our study showed that, in the future, there ~~will-would~~ be  
397 an increase in surge level from a minimum of ~~13.725%~~ up to ~~5570%~~ if a TC 1 or a TC 5 makes landfall under increased SLR  
398 conditions (~~Table 6, Table 7~~). So, the authority may consider increasing the height of the first floor considering the future risk of  
399 an increase in storm surge level and safety of local populations. Also, our model outputs showed that the inundated area increase  
400 would range from ~~28.3%-53%~~ (~~Table 5~~) ~~percent~~ if there's any TC 1 or TC 5 was to make landfall with SLRs of 0.26 m or 0.54 m.  
401 This shows that a huge number of new areas are going to face the impacts of storm surge inundation and by considering this issue,  
402 it is high time to increase the number of TC shelters in the coastal areas of Bangladesh.

## 403 5. Conclusion

404

405  
406 Employing the Delft3D-FLOW model, we simulated coastal storm surge and inundation for ~~present-daypresent-day~~ and future  
407 SLR scenarios and compared the changes between them. After validating the ~~present-daypresent-day~~ model, simulations were  
408 conducted for mid-21<sup>st</sup>-~~century-century~~ and end-of-21<sup>st</sup>-~~century-century~~ climate scenarios where the SLR has been considered as  
409 0.26 m and 0.54 m respectively. The model results showed that, with an increase of 0.26 m and 0.54 m SLR, there would be an  
410 increase of ~~318%~~ and ~~5348%~~ of inundated area respectively if TC Sidr was to made landfall with its ~~present-daypresent-day~~  
411 strength. There would also be an increase of ~~28.35%~~ and ~~46.534%~~ in inundated area if ~~categoryCategory-1~~ TC Aila would make  
412 landfall with its ~~present-daypresent-day~~ strength but under the condition of 0.26 m and 0.54 m respectively. Outputs from the  
413 ensemble projections showed that, even if the TC intensities, landfall location and timings are uncertain, the most probable range  
414 of inundated area a extent would shift from 1000-1250 km<sup>2</sup> (present day) to 2000-2250 km<sup>2</sup> (0.26 ~~meterm~~ SLR) and 3500-3750 km<sup>2</sup>  
415 (0.54 ~~meterm~~ SLR). Besides the inundated area, we also investigated the changes in storm surge level if TC Sidr and TC Aila  
416 would make landfall under future SLR conditions. Similar to the inundated area, increases in storm surge levels were found for  
417 future scenarios. The significant increase in simulated storm surge and inundation hazards highlights the need for the local  
418 governments to improve cyclone preparedness in future SLR scenarios.

## 419 Acknowledgement

420 The authors would like to thank Coastal Carolina University's Cyber-infrastructure project (<http://ci.coastal.edu>) for providing  
421 access to computational resources. Also, we would like to acknowledge Dr. Susan Kay from Plymouth Marine Laboratory, UK  
422 for her thoughtful opinions regarding the SLR input in model and Institute of Water and Flood Management, Bangladesh for

423 providing important data ~~&~~and support for this work. [The authors also appreciate the helpful comments and suggestions from](#)  
424 [the three anonymous reviewers.](#)

## 425 **References:**

426 Ali, A.: Vulnerability of Bangladesh to climate change and sea level rise through tropical cyclones and storm surges, *Climate*  
427 *Change Vulnerability and Adaptation in Asia and the Pacific*, Springer, pp. 171–179., doi: 10.1007/978 94-017-1053-4\_16, 1996.

428 ~~Alam, M.: Subsidence of the Ganges—Brahmaputra delta of Bangladesh and associated drainage, sedimentation and salinity~~  
429 ~~problems, *Sea Level Rise and Coastal Subsidence*, Springer, pp. 169–192, doi:10.1007/978 94 015 8719 8\_9, 1996.~~

430 Bender, M.A., Knutson, T.R., Tuleya, R.E., Sirutis, J.J., Vecchi, G.A., Garner, S.T., Held, I.M.: Modeled impact of  
431 anthropogenic warming on the frequency of intense Atlantic hurricanes, *Science*, 327, 454–458, doi: 10.1126/science.1180568,  
432 2010.

433 Bengtsson, L., Hodges, K.I., Esch, M., Keenlyside, N., Kornblueh, L., LUO, J.-J., Yamagata, T.: How may tropical cyclones  
434 change in a warmer climate?, *Tellus a*, 59, 539–561, doi: 10.1111/j.1600-0870.2007.00251.x, 2007.

435 BODC.: Centenary Edition of the GEBCO Digital Atlas, published on CD-ROM on behalf of the Intergovernmental  
436 Oceanographic Commission and the International Hydrographic Organization as part of the General Bathymetric Chart of the  
437 Oceans. British oceanographic data centre, Liverpool, 2003.

438 Caesar, J., Janes, T., Lindsay, A.: Climate projections over Bangladesh and the upstream Ganges-Brahmaputra-Meghna system,  
439 under review, *Environmental Science: Processes & Impacts (Under Review)*, 2017.

440 ~~Delft Hydraulics~~~~Hydraulics, D.:~~ Delft3D-FLOW user manual. Delft, the Netherlands, 2006.

441 ~~Delft Hydraulics.:Wind Enhancement Scheme for cyclone modelling, 2011.~~

443 Egbert, G. D., Bennett, A. F. and Foreman, M. G. G.: TOPEX/POSEIDON tides estimated using a global inverse model, *J.*  
444 *Geophys. Res.*, 99(C12), 24821–24852, doi:10.1029/94JC01894, 1994.

445 Goodbred, S.L., Kuehl, S.A., Steckler, M.S., Sarker, M.H.: Controls on facies distribution and stratigraphic preservation in the  
446 Ganges–Brahmaputra delta sequence, *Sedimentary Geology*, 155, 301–316, doi:10.1016/S0037-0738(02)00184-7, 2003.

447 Haarsma, R.J., Hazeleger, W., Severijns, C., Vries, H., Sterl, A., Bintanja, R., Oldenborgh, G.J., Brink, H.W.: More hurricanes to  
448 hit western Europe due to global warming, *Geophysical Research Letters*, 40, 1783–1788, doi: 10.1002/grl.50360, 2013.

449 Haque, C.E.: Atmospheric hazards preparedness in Bangladesh: a study of warning, adjustments and recovery from the April  
450 1991 cyclone, *Earthquake and Atmospheric Hazards*, Springer, pp. 181–202, doi: 10.1007/978-94-011-5034-7\_6, 1997.

451 Harris, D. L.: Characteristics of the hurricane storm surge, Tech. Pap., 48, U. S. Weather Bur., Washington, D. C., 139 pp, 1963.

452 Hearn, C. J.: *The dynamics of coastal models*. Cambridge University Press, 2008.

453 Heming, J. T., Chan, J. C. L. and Radford, A. M.: A new scheme for the initialization of tropical cyclones in the UK  
454 Meteorological Office global model, *Met. Apps*, 2, 171–184, doi:10.1002/met.5060020211, 1995.

455 Holland, G. J.: An analytic model of the wind and pressure profiles in hurricanes, *Monthly weather review*, 108(8), 1212-1218,  
456 doi:10.1175/1520-0493(1980)108<1212:AAMOTW>2.0.CO;2, 1980.

457 Karim, M.F., Mimura, N.: Impacts of climate change and sea-level rise on cyclonic storm surge floods in Bangladesh, *Global*  
458 *Environmental Change*, 18, 490–500, doi: 10.1016/j.gloenvcha.2008.05.002, 2008.

- 459 Knutson, T.R., McBride, J.L., Chan, J., Emanuel, K., Holland, G., Landsea, C., Held, I., Kossin, J.P., Srivastava, A.K., Sugi, M.:  
460 Tropical cyclones and climate change, *Nature Geoscience*, 3, 157–163, doi: 10.1038/ngeo779, 2010.
- 461 Meehl, G.A., Covey, C., Delworth, T., Latif, M., McAvaney, B., Mitchell, J.F.B., Stouffer, R.J., Taylor, K.E., and Coauthors, :  
462 Global climate projections. *Climate Change 2007: The Physical Science Basis*, S. Solomon et al., Eds. Cambridge University  
463 Press, 2007.
- 464 Milliman, John D., James M. Broadus, and Frank Gable.: Environmental and economic implications of rising sea level and  
465 subsiding deltas: the Nile and Bengal examples, *Ambio*, 18 (6), 340-345, doi: , 1989.
- 466 ~~Mohal, N., Khan, Z.H., Rahman, N., 2006. Impact of sea level rise on coastal rivers of Bangladesh. Dhaka: Institute of Water  
467 Modelling (IWM). Assessment conducted for WARPO, an organization under Ministry of Water Resources.~~
- 468 Mukhopadhyay, A., Mondal, P., Barik, J., Chowdhury, S.M., Ghosh, T., Hazra, S.: Changes in mangrove species assemblages and  
469 future prediction of the Bangladesh Sundarbans using Markov chain model and cellular automata, *Environmental Science:  
470 Processes & Impacts*, 17, 1111–1117, doi: 10.1039/C4EM00611A, 2015
- 471 Murty, T.S., Flather, R.A., Henry, R.F.: The storm surge problem in the Bay of Bengal. *Progress in Oceanography*, 16, 195–233,  
472 doi: 10.1016/0079-6611(86)90039-X ,1986.
- 473 Nash, J.E., Sutcliffe, J.V.:River flow forecasting through conceptual models part I—A discussion of principles, *Journal of  
474 hydrology*, 10, 282–290, doi:10.1016/0022-1694(70)90255-6, 1970.
- 475 Pietrafesa, L. J., Janowitz, G. S., Chao, T. Y., Weisberg, R. H., Askari, F., & Noble, E.: The physical oceanography of Pamlico  
476 Sound. University of North Carolina Sea Grant Publication UNC-WP-86-5, Raleigh, North Carolina, 125, 1986
- 477 Pietrafesa, L.J., Bao, S., Yan, T., Slattery, M., Gayes, P.T.: On Sea Level Variability and Trends in United States Coastal Waters  
478 and Relationships with Climate Factors, *Advances in Adaptive Data Analysis*, 7, 1550005, doi: 10.1142/S1793536915500053,  
479 2015.
- 480 [Pickering, M. D., Wells, N.C., Horsburgh, K. J., and Green, J. A. M.: The impact of future sea-level rise on the European Shelf  
481 tides. \*Continental Shelf Research\* 35: 1-15, doi:10.1016/j.csr.2011.11.011, 2012.](#)
- 482 Sakib, M., Nihal, F., Haque, A., Rahman, M., Ali, M.: Sundarban as a Buffer against Storm Surge Flooding, *World Journal of  
483 Engineering and Technology*, 3, 59, doi: 10.4236/wjet.2015.33C009, 2015.
- 484 SMRC.: The Vulnerability Assessment of the SAARC Coastal Region due to Sea Level Rise: Bangladesh Case, SAARC  
485 Meteorological Research Center, Dhaka SMRC-No. 3, 2003.
- 486 Vatvani, D.K., Gerritsen, H., Stelling, G. S., Rao, A. K.: Cyclone induced storm surge and flood forecasting system for India.  
487 *Solutions to Coastal Disasters '02*, San Diego, CA, 2002.
- 488 Warrick, R.A., Bhuiya, A.A.H., Mitchell, W.M., Murty, T.S., Rasheed, K.B.S.: Sea-level Changes in the Bay of Bengal, in: *The  
489 Implications of Climate and Sea–Level Change for Bangladesh*, Springer, pp. 97–142, 1996.
- 490 Whitehead, P.G., Barbour, E., Futter, M.N., Sarkar, S., Rodda, H., Caesar, J., Butterfield, D., Jin, L., Sinha, R., Nicholls, R., others.:  
491 Impacts of climate change and socio-economic scenarios on flow and water quality of the Ganges, Brahmaputra and Meghna  
492 (GBM) river systems: low flow and flood statistics, *Environmental Science: Processes & Impacts*, 17, 1057–1069, doi:  
493 10.1039/C4EM00619D, 2015.
- 494 Xie, L., Bao, S., Pietrafesa, L.J., Foley, K., Fuentes, M.: A real-time hurricane surface wind forecasting model: Formulation and  
495 verification, *Monthly Weather Review*, 134, 1355–1370, doi:10.1175/MWR3126.1, 2006.
- 496 Zhang, K., Liu, H., Li, Y., Xu, H., Shen, J., Rhome, J., Smith, T.J.: The role of mangroves in attenuating storm surges, *Estuarine,  
497 Coastal and Shelf Science* 102, 11–23, doi: 10.1016/j.ecss.2012.02.021, 2012.

498

499

500

501

502

503

504

505

506

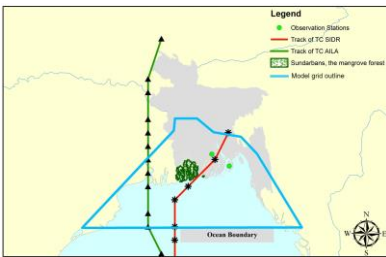
507

508

509

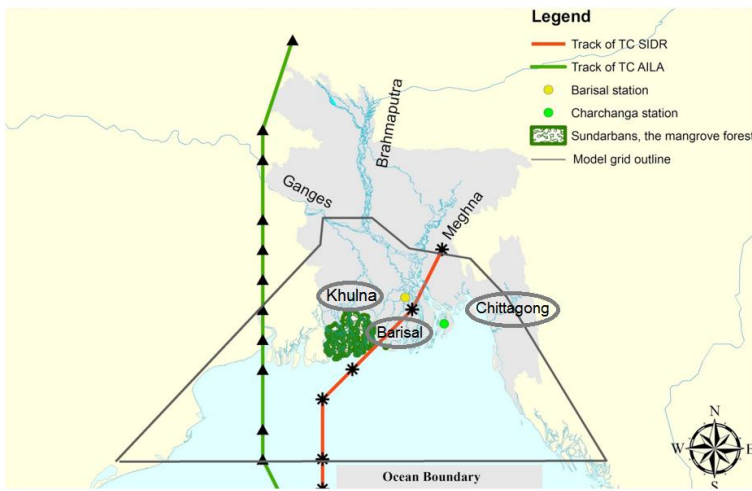
510

511

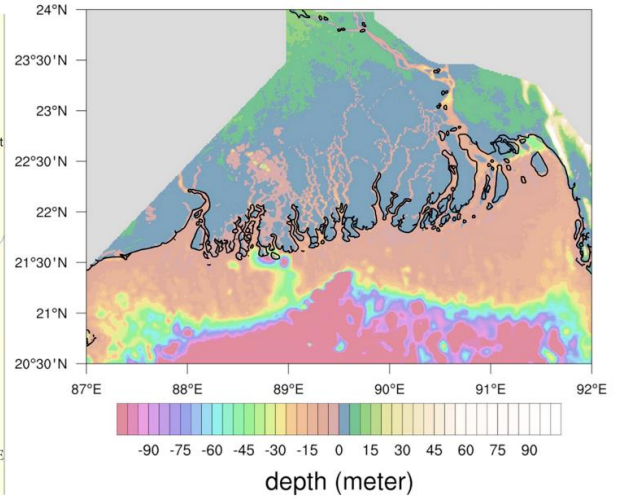


516

(a) Study Area



(b) Topography and Bathymetry



517

518

519 **Figure 1.** (a) Map showing of the study area for this work. The red and green lines representing the tracks of TC Sidr and TC Aila respectively.  
520 The Area area marked with green color indicates the Sundarban mangrove forest region. Location of the Ganges, Brahmaputra and Meghna rivers  
521 are shown on the map. Khulna, Barisal and Chittagong which are landfall locations for the historical TCs used for ensemble projection, shown  
522 inside a circular box on the map. Two green circles over the study area are the observation stations of Bangladesh Inland Water Transport  
523 Authority (BIWTA). The blue-black colored outline shows the extent of model grid over the region. (b) Topography and bathymetry of the model  
524 domain. Negative depth values are representing water bodies (ocean and rivers) and positive depth values areas representing land.

525

526

527

528

529

530



531

532

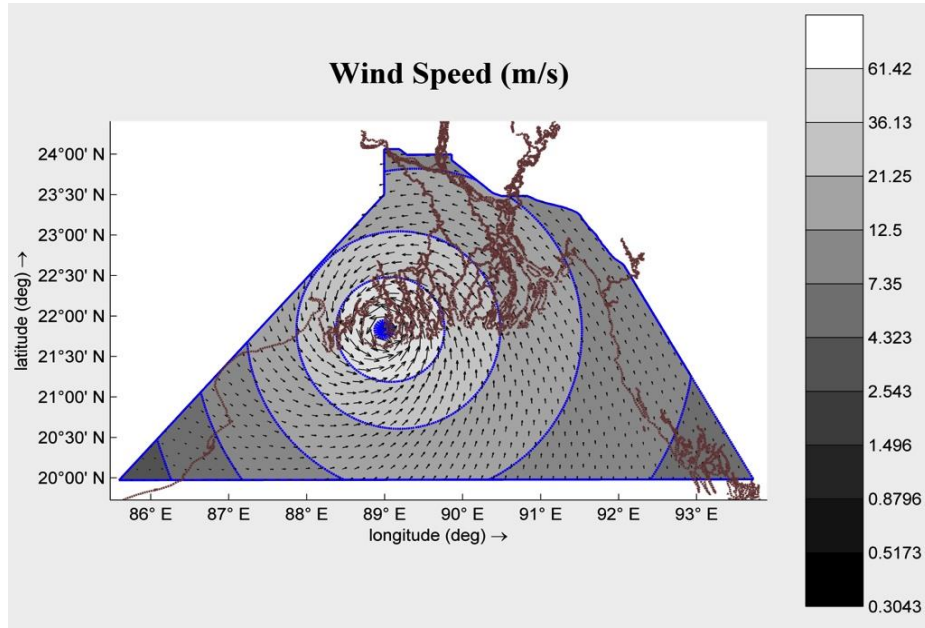


**Figure 2.** Distribution of the wind field over the model domain for TC Sidr during landfall generated using Holland's Equation.

533

534

535

536

537

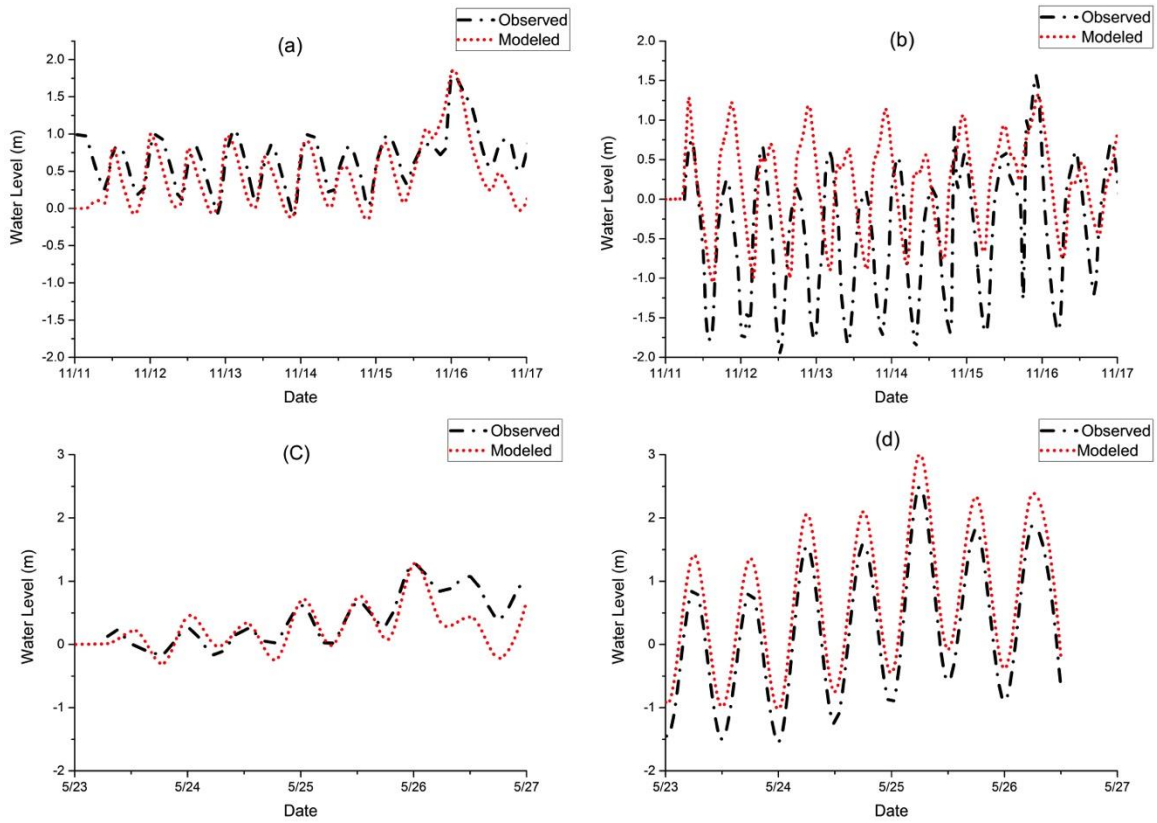
538

539

540

541

542



543

544

545

546

547

548

549

550

551

552

553

554

**Figure 3.** Comparison of observed and modeled Water Level for TC Sidr and TC Aila in Barisal and Charchanga observation stations. (a) mMeasured and Modeled Water Level comparison for TC Sidr in Barisal; (b) Mmeasured and Modeled Water Level comparison for TC Sidr in Charchanga; (c) Mmeasured and Modeled Water Level comparison for TC Aila in Barisal; (d) Mmeasured and Modeled Water Level comparison for TC Aila in Charchanga.

### Comparison of Inundated Area between TC Sidr and TC Aila under Present Day Scenario

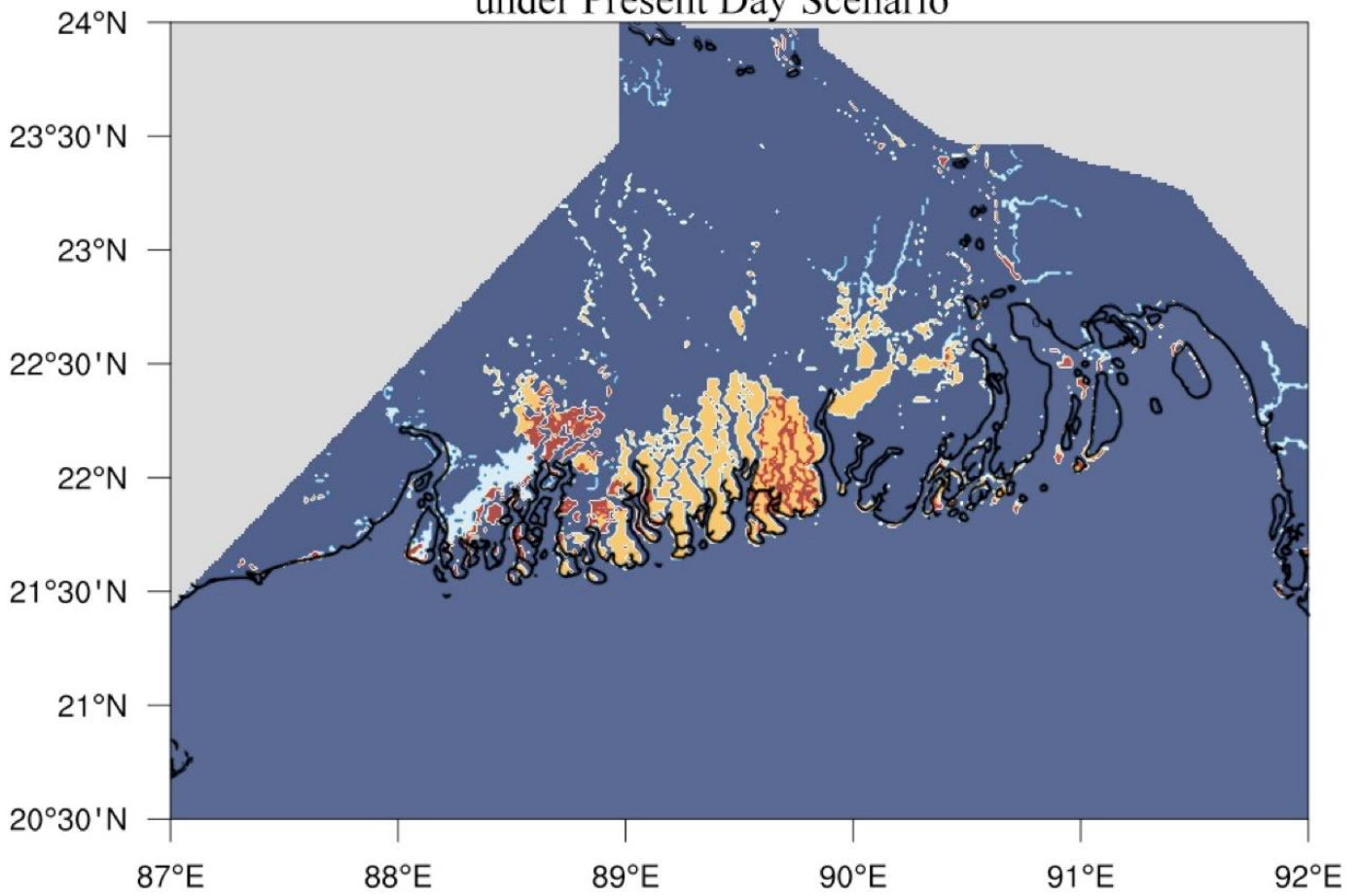


**Figure 4.** Yellow colors denotes the areas flooded by TC Sidr but not in Aila, and the white color representing the area inundated by TC Aila but not in Sidr. Red color is the area flooded by both TC Sidr and TC Aila. Blue color is showing the non-flooded area (either land or constant water).

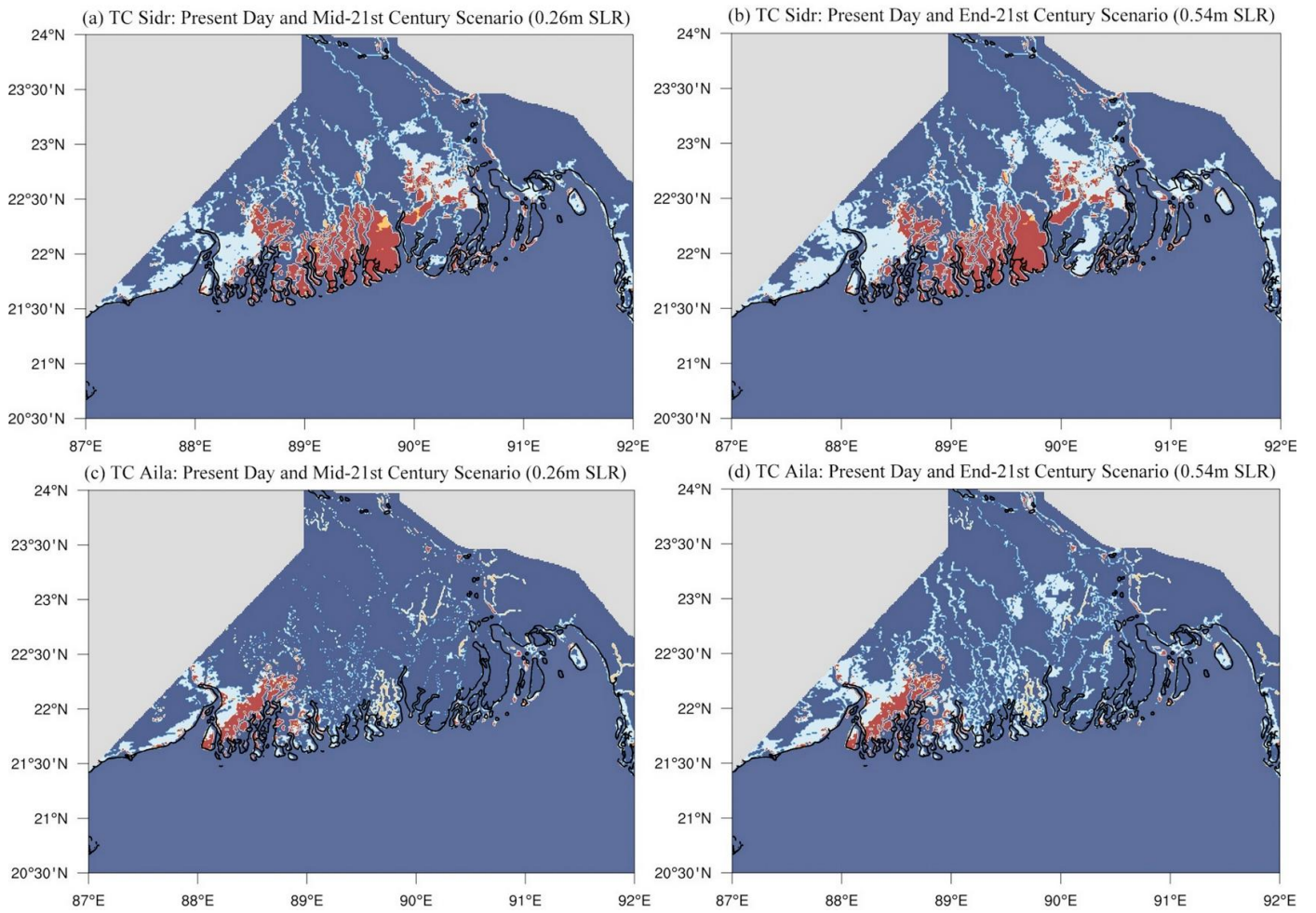
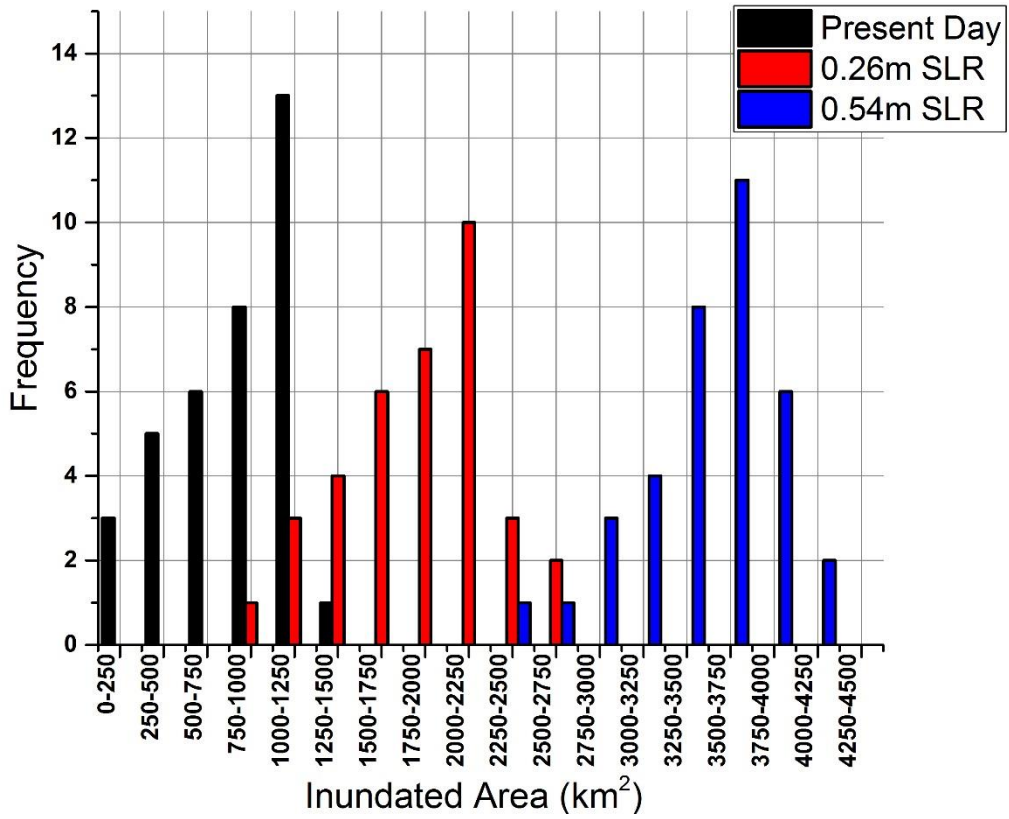


**Figure 5:** Comparison of inundated area between ~~present-day~~ present-day and future climate scenarios for (a) TC Sidr mid-21<sup>st</sup> century 0.26m SLR (b) TC Sidr end-21<sup>st</sup> century 0.54m SLR (c) TC Aila mid-21<sup>st</sup> century 0.26m SLR (d) TC Aila end-21<sup>st</sup> century 0.54m SLR. White color is representing the increased flooded areas that were not in ~~present-day~~ present-day scenario but the increase due to future SLR. Red color is showing the inundated areas that were similar both for

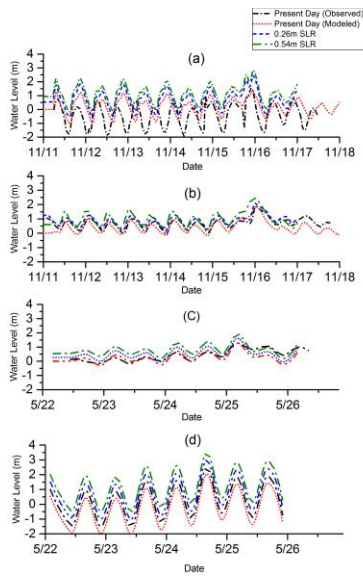
567  
568  
569  
570  
571  
572



573

574 **Figure 6:** Ensemble projection of the future SLR impact on storm surge inundation. The column in black color is representing the inundation  
 575 events for present-day sea level condition, red colored one is for 0.26 meter of SLR and blue colored column is for 0.54 meter of  
 576 SLR conditions. In total 108 simulations were conducted for present and two future SLR scenarios.

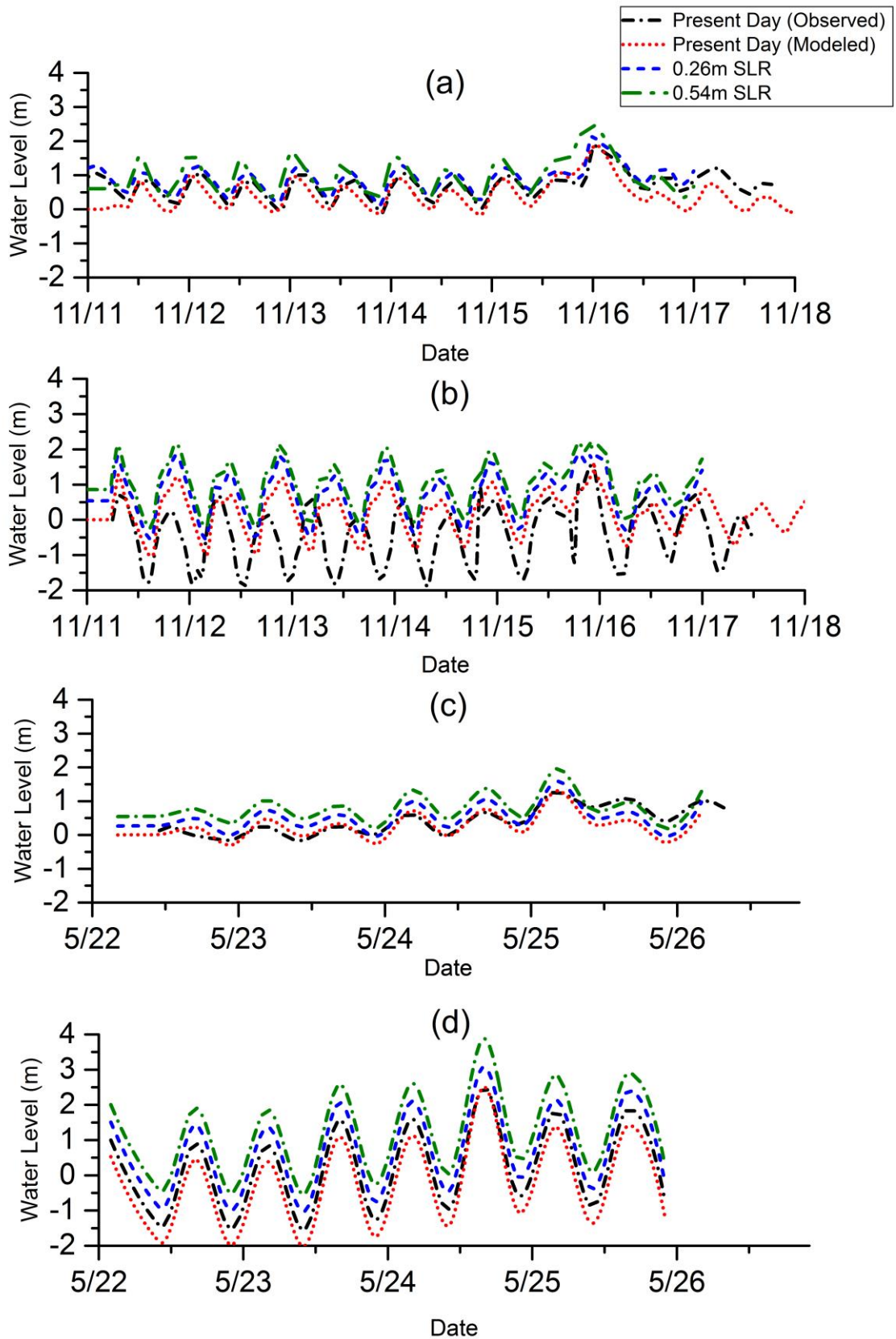
577



578

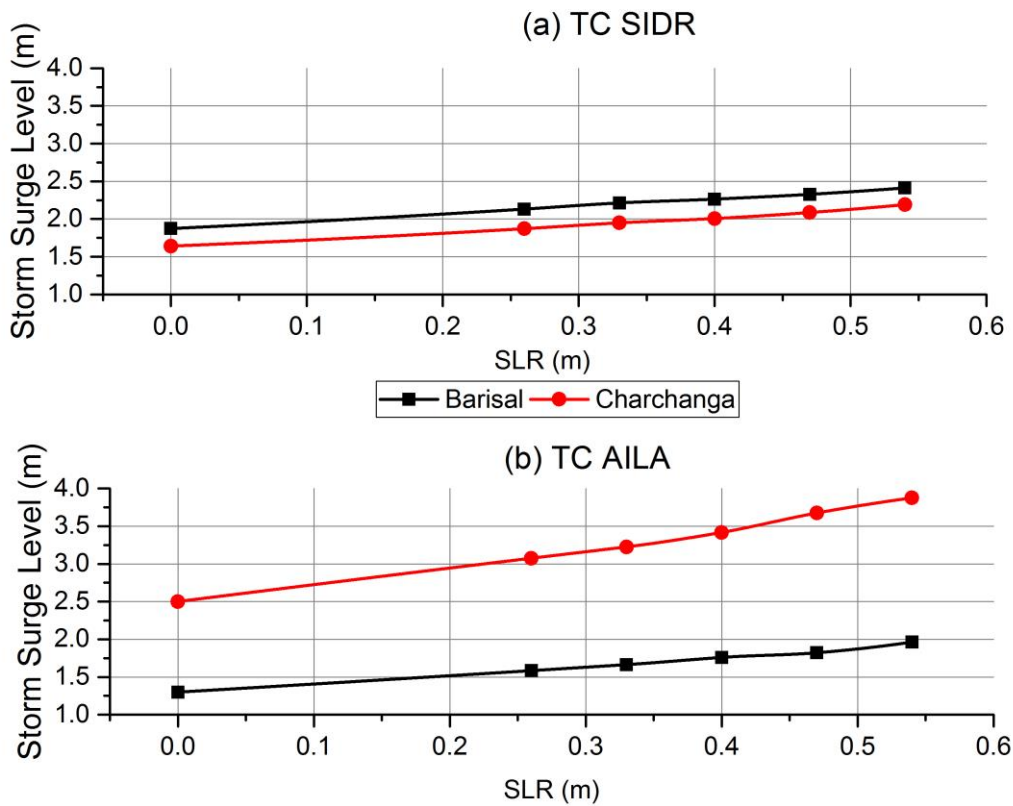
579

580



581

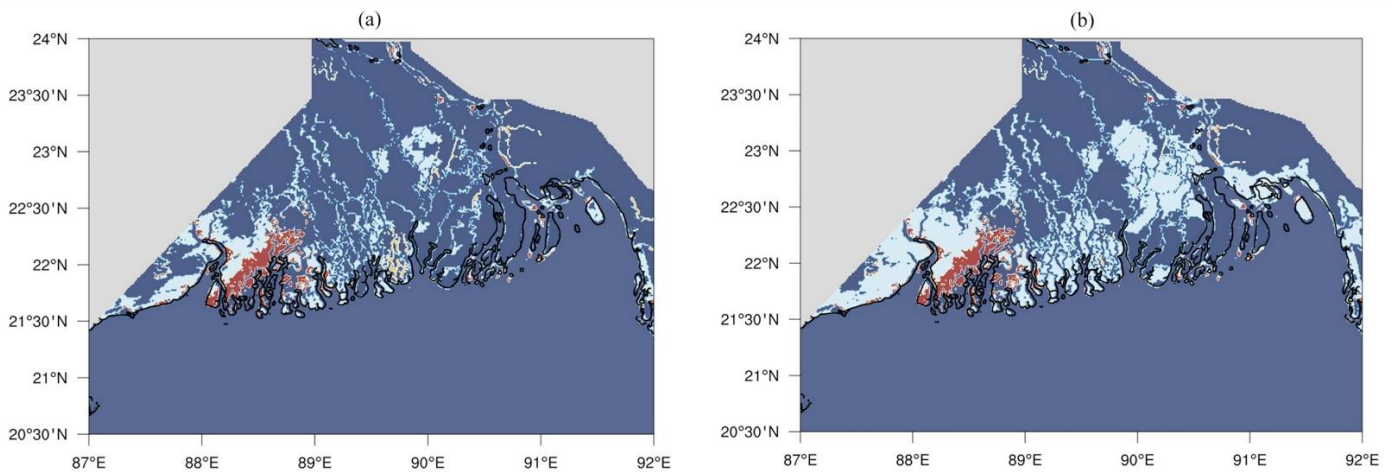
582 **Figure 7.** Comparison of storm surge water levels between present-day and future SLR scenarios. (a) TC Sidr at Barisal (b) TC Sidr  
 583 at Charchanga (c) TC Aila at Barisal (d) TC Aila at Charchanga. The observed, modeled present-day, mid-of-21<sup>st</sup>-century and end-of-  
 584 21<sup>st</sup>-century storm surge levels are denoted by the black dash-dotted, red dashed-dotted, blue dotted-dashed, and green dash-  
 585 dotted lines, respectively.



587

588 **Figure 8.** Relation between SLR and increase in storm surge level with respect to the present-day present-day simulated water level for the case  
 589 of TC Sidr and TC Aila. (a) is representing the relation for TC Sidr and (b) is representing the relation for TC Aila.

590



591

592 **Figure 89.** Comparison of inundated areas for TC Aila between present-day present-day and end-21<sup>st</sup>-21<sup>st</sup>-century (0.54m SLR) scenario. White  
 593 color is representing the increased flooded areas that were not in present-day present-day scenario but the increase due to future SLR. -Red color  
 594 is showing the inundated area that's similar both for present-day present-day and future scenario case. Blue areas are either land or constant waters  
 595 (those which are already water at the model initialization time). Figure (a) is representing the inundated area when SLR was considered on ocean  
 596 depths instead of adding it in to the open ocean boundary and figure-figure (b) is showing the inundated area when we considered the SLR on  
 597 ocean boundary.

598

599

600

**Table 1** Manning’s Roughness Coefficient for different land coverings.

Land cover	Manning’s coefficient
River	0.015
Mangrove	0.080
Ocean	0.01
Land	0.025

601

602

**Table 2** List of 12 historical TC events used for ensemble projection of storm surge inundation

603

<u>Name</u>	<u>Date</u>	<u>Landfall location</u>
<u>Tropical storm 13</u>	<u>14-18 November, 1973</u>	<u>Noakhali</u>
<u>Cyclone 12</u>	<u>23-28 November, 1974</u>	<u>Bhola</u>
<u>Tropical storm 19</u>	<u>07-12 November, 1975</u>	<u>Chittagong</u>
<u>Tropical storm 1</u>	<u>22-25 May, 1985</u>	<u>Noakhali</u>
<u>Cyclone 4</u>	<u>21-30 November, 1988</u>	<u>Khulna</u>
<u>Cyclone 2</u>	<u>22-30 April, 1991</u>	<u>Chittagong</u>
<u>Cyclone 2</u>	<u>26 April – 30 May, 1994</u>	<u>Cox’s Bazar</u>
<u>Cyclone 4</u>	<u>18-25 November, 1995</u>	<u>Cox’s Bazar</u>
<u>Cyclone 1</u>	<u>13-20 May, 1997</u>	<u>Noakhali</u>
<u>Tropical storm 4</u>	<u>24-27 October, 2008</u>	<u>Barguna</u>
<u>Tropical storm Mahasen</u>	<u>10-16 May, 2013</u>	<u>Patuakhali</u>
<u>Tropical storm Roanu</u>	<u>18-21 May, 2016</u>	<u>Chittagong</u>

604

605

606

607



609 **Table 32:** Parameters considered for ensemble projection of storm surge inundation which includes the TC intensities, tidal conditions and the  
610 SLR scenarios.

TC name	Intensities	Tide conditions	SLR
TC Sidr	+10%, present day, -10%	High Tide, low tide, actual tide, zero tide	Present day, 0.26 <del>meter</del> m, 0.54 <del>meter</del> m
TC Aila	+10%, Present day, -10%	High Tide, low tide, actual tide, zero tide	Present day, 0.26 <del>meter</del> m, 0.54 <del>meter</del> m
12 historical TC tracks	Actual intensities	Actual tide conditions	Present day, 0.26 <del>meter</del> m, 0.54 <del>meter</del> m

611

612 **Table 43.** Computed values of RMSE, MAE and Nash-Sutcliffe coefficient for both TC Sidr and TC Aila

Stations	TC Sidr			TC Aila		
	RMSE (m)	MAE (m)	NASH	RMSE (m)	MAE (m)	NASH
Barisal	0.23	0.16	0.85	0.33	0.24	0.65
Charchanga	0.26	0.19	0.80	0.28	0.17	0.73
<b>Average</b>	<b>0.245</b>	<b>0.175</b>	<b>0.825</b>	<b>0.305</b>	<b>0.205</b>	<b>0.69</b>

613

614 **Table 5.** Comparison of inundated area between ~~present day~~present-day & future SLR scenarios and calculated change in percentage with  
615 respect to ~~present day~~present-day scenario.

616

<u>Scenario</u>	<u>TC Sidr</u>		<u>TC Aila</u>	
	<u>Inundated Area (km<sup>2</sup>)</u>	<u>(%) increase</u>	<u>Inundated Area (km<sup>2</sup>)</u>	<u>(%) increase</u>
<u>Present-day</u>	<u>1860</u>		<u>1208</u>	
<u>Mid-21<sup>st</sup>-century</u>	<u>2436.6</u>	<u>+31</u>	<u>1550</u>	<u>+28.3</u>
<u>End-21<sup>st</sup>-century</u>	<u>2845.8</u>	<u>+53</u>	<u>1770</u>	<u>+46.5</u>

617

618

619

620

**Table 6.** Comparison of storm surge level between present-day and future SLR scenarios for the case of TC Sidr

<u>Scenario</u>	<u>Barisal</u>		<u>Charchanga</u>	
	<u>Storm surge level (m)</u>	<u>% increase</u>	<u>Storm surge level (m)</u>	<u>% increase</u>
<u>Present Day</u> Present-day	<u>1.873</u>		<u>1.641</u>	
<u>Mid-21<sup>st</sup>-century (0.26m)</u>	<u>2.13</u>	<u>13.72</u>	<u>1.870</u>	<u>13.95</u>
<u>End-21<sup>st</sup>-century (0.54m)</u>	<u>2.41</u>	<u>28.67</u>	<u>2.19</u>	<u>33.45</u>

621

622

**Table 7.** Comparison of storm surge level between ~~present-day~~present-day and future SLR scenarios for the case of TC Aila

<u>Scenario</u>	<u>Barisal</u>		<u>Charchanga</u>	
	<u>Storm surge level (m)</u>	<u>% increase</u>	<u>Storm surge level (m)</u>	<u>% increase</u>
<u>Present Day</u> Present-day	<u>1.299</u>		<u>2.5</u>	
<u>Mid-21<sup>st</sup>-century (0.26m)</u>	<u>1.584</u>	<u>21.93</u>	<u>3.075</u>	<u>23</u>
<u>End-21<sup>st</sup>-century (0.54m)</u>	<u>1.961</u>	<u>50.96</u>	<u>3.875</u>	<u>55</u>

623